Research Paper

The Holocene
1–13

DOI: 10.1177/09596836231211807
journals.sagepub.com/home/hol
Sage

Assessing atmospheric and oceanic teleconnections between the eastern and western Mediterranean over the past 8000 years

Sandrine Le Houedec,[1] Diederik Liebrand,[2,3] Rick Hennekam[4] and Meryem Mojtahid[5]

Abstract

Holocene climate records from the Mediterranean are marked by pervasive millennial to centennial-scale climate variability. Here, we investigate East-West Mediterranean atmospheric and oceanic teleconnections by computing phase-relationships between oxygen isotope ($\delta^{18}O$) records generated on Soreq (East) and Chorchia (West) spelaeothems, as well as between $\delta^{18}O$ and carbon isotope ($\delta^{13}C$) records from planktonic and benthic foraminifera from core PS009PC (East, Levantin Basin), ODP Site 963D (Central, Sicily Strait), and core KESC9-14 (West, Ligurian Basin). These marine sites are all located at intermediate water depths (560–460 m depth). Hence, the benthic foraminiferal $\delta^{18}O$ records reflect mainly the intermediate ocean temperature/$\delta^{18}O$ of the water mass, and the benthic $\delta^{13}C$ is a proxy for the intensity of water flowing at the studied depth called Levantine Intermediate Water (LIW). For both western and eastern cores, the planktonic stable isotopic records reflect the climate-induced activity of the nearby river system. We find broadly in-phase relationships between the spelaeothem $\delta^{18}O$ records and between the planktonic $\delta^{18}O$ and $\delta^{13}C$ records at most multi-centennial and millennial periodicities. This is indicative of closely linked (hydro-) climatic conditions in Southern Europe, the Levant, and North Africa over the last 8000 years. Conversely, at intermediate water depths, we find a distinct out-of-phase relationship between the East/Central and West Mediterranean benthic $\delta^{18}O$ and $\delta^{13}C$ records at 1000–2000 years periodicities. We interpret this see-saw pattern as indicative of a persistent regional influence of LIW on oceanographic conditions in the intermediate depths of the eastern basin. Conversely, we suggest a strong influence of the modified Atlantic Ocean inflow (MAW) in the intermediate water formation in the Western Mediterranean ('Winter Intermediate Water'; WIW). This WIW overprints, at least partially, the LIW signal that reaches the western Mediterranean causing the out-of-phase relationship between the east and the west oceanographic signals at intermediate depths.

Keywords

E-W teleconnection, Holocene, Levantine intermediate water, Mediterranean Sea, Paleocirculation, spectral analyses

Received 20 February 2023; revised manuscript accepted 25 August 2023

Introduction

Climate change is already having substantial physical impacts that affect natural and socioeconomic systems across the world, and yet may facets of the intricate climate machinery still challenge the research community. Amongst the many gaps in our knowledge of the functioning of the climate system, the role of ocean-atmosphere exchanges, the most dynamic component of the climate, remains poorly understood (e.g. Bye, 1996; Cabos et al., 2020; Christensen et al., 2013). The last 8 kyrs are of particular interest because orbital forcing, operating at multi-millennial timescales, is no longer the only major controlling factor (Clark et al., 2016). The composite effects of external factors (e.g. volcanic, solar and orbital) and feedbacks in the climate system (internal forcing) become fundamental (e.g. Morley et al., 2014).

To assess the significance of ongoing climate change and future projections it is crucial to understand the long-term trends and spatial patterns of climate variability in the current interglacial period, the Holocene. Due to its small volume-to-surface area ratio, the Mediterranean Sea tends to respond to climate change, and to changes in freshwater inputs via evaporation, precipitation, and river runoff, much more strongly than the open ocean (MedECC, 2020). Therefore, the Mediterranean Sea has a much shorter turnover rate (about one-tenth) compared to the global ocean (Schroeder et al., 2016), which makes the water mass particularly sensitive to ocean-atmosphere exchanges and thus should have a high potential to respond to the millennial

[1]Department of Earth Sciences, University of Geneva, Switzerland
[2]British Ocean Sediment Core Research Facility (BOSCORF), National Oceanography Centre, Southampton, UK
[3]Department of Earth and Environmental Sciences, The University of Manchester, UK
[4]Department of Ocean Systems, NIOZ Royal Netherlands Institute for Sea Research, The Netherlands
[5]Univ Angers, Nantes Université, Le Mans Université, CNRS, UMR 6112, Laboratoire de Planétologie et Géosciences, France

Corresponding author:
Sandrine Le Houedec, Department of Earth Sciences, University of Geneva, Rue des Maraîchers 13, Genève CH-1205, Switzerland.
Email: sandrine.lehouedec@unige.ch

Holocene climatic variability. Consequently, the Mediterranean Sea was repeatedly highlighted as particularly sensitive to human-induced global warming by the successive Intergovernmental Panel on Climate Change (IPCC) reports (AR5, AR6). For instance, the warming of the circum-Mediterranean has been shown to be about 20% above the global average (e.g. Jia et al., 2019; Mirzabaev et al., 2019; Stocker et al., 2013). Lower mean precipitation, increased chance of flash floods, greater aridity, drought, and water scarcity (among other impacts) have been projected for the Mediterranean surrounding countries under continued fossil fuel emissions (IPCC, AR6, working group 1, Masson-Delmotte et al., 2021). Thus, understanding the low frequency (millennial) component of past climate change is important to study the mechanisms of the natural (hydro) climate variability of the circum-Mediterranean area, and the regional specificities within this area, which is ultimately essential to improved predictions on all timescales.

In the case of the Mediterranean region, most of the cyclic climatic patterns recognized at sub-Milankovitch timescales (<20 ka) during the late Pleistocene and Holocene were mostly related with Dansgaard–Oeschger (D–O) oscillations and Heinrich events (e.g. Cacho et al., 1999, 2000, 2001; Martrat et al., 2004; Moreno et al., 2005; Naughton et al., 2009; Shackleton et al., 2000; Sierro et al., 2005; Sprovieri et al., 2012). This demonstrates the strong link between the Mediterranean Sea, the North Atlantic climates, and the African monsoon regimen (e.g. Sánchez Goñi et al., 2008; Sprovieri et al., 2012). Another set of millennial warm/cold and humid/arid climate shifts is also frequently recorded in many marine and continental records of the western-central Mediterranean regions (Desprat et al., 2013; Di Rita et al., 2018; Magny et al., 2013; Rodrigo-Gámiz et al., 2014) and were linked to the pervasive 1500 ± 300 year-Bond cycles. However, while it is well-known that the Holocene exhibits a millennial-scale climate variability over the Mediterranean Sea, the spatio-temporal patterns and underlying processes are not fully deciphered yet. For instance, in the central Mediterranean, terrestrial records show North-South palaeohydrological contrasts (Magny et al., 2013) which are interpreted as latitudinal shifts in response to changing NAO (North Atlantic Oscillation) phases. Also, even if it is still debated, some authors assess the existence of a Mediterranean Oscillation (MO) with opposed precipitation and/or temperature anomalies between the northwestern and southeastern basins (Conte et al., 1989; Dünkeloh and Jacobeit, 2003; Fletcher et al., 2013; Palutikof et al., 1996) suggested to result of an NAO teleconnection over the last century (Roberts et al., 2012). However, from those studies, none explore the possible expression/connection of those Holocene millennial cycles on/with the marine realm.

In the Mediterranean Sea, a direct consequence of the atmosphere-sea exchanges is the modulation of the flow rate/production of the modern intermediate Mediterranean waters (LIW and WIW). For instance, the production rate of LIW was shown to be affected by the amount of freshwater input to the eastern basin from the Nile River ultimately controlled by the East Africa/Indian monsoonal activity at year to centennial time scales and thus to the seasonal climatic variability (Hennekam et al., 2014; Incarbona and Sprovieri, 2020; Mojtahid et al., 2015; Rohling et al., 2015). On orbital time scales, a similarly persistent monsoonal forcing controls the amount of Mediterranean Outflow Water, which is also governed by LIW production in the eastern basin (Bahr et al., 2015). Another mechanism implied in the modulation of the production rate of the LIW is the outbreaks of cold and dry air into the Levantine basin from the northern continental regions. Those winds cool the surface saline waters causing occasional downwelling in the Rhodes Gyre, which forms the Levantine intermediate water (LIW, Figure 1). In the western basin, an additional intermediate water, the Winter intermediate water (WIW) (Juza et al., 2013, 2019; Petrenko, 2003; Salat and Font, 1987) is also produced under strong north westerly winds cooling

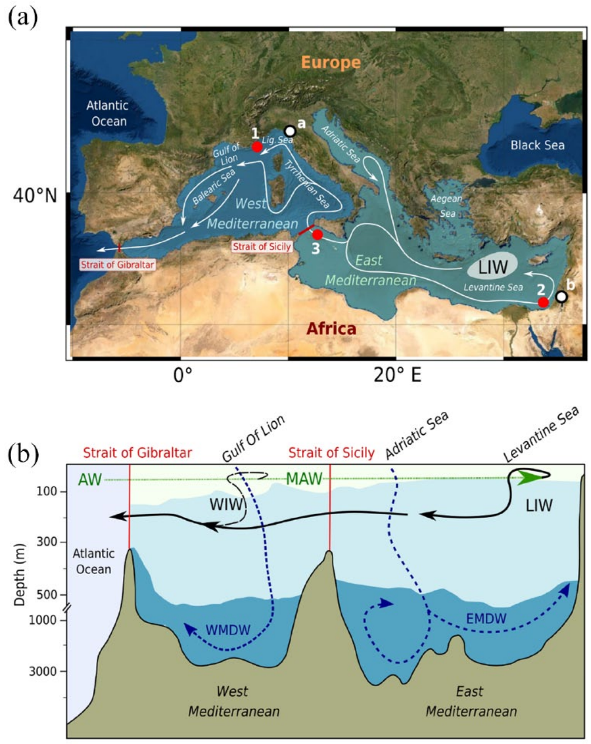

Figure 1. (a) Map of the region with site locations. For marine sediment cores, number 1 corresponds to the western Mediterranean Core KESC9-14, number 2 indicates eastern Mediterranean Core PS009PC and number 3 the central Mediterranean Site ODP 963 (Incarbona and Sprovieri, 2020). For the cave spelaeothems, Site 'a' marks the position of the Corchia Cave spelaeothem (Bar-Matthews and Ayalon, 2011), and Site 'b' displays the position of the Soreq Cave spelaeothem (Zanchetta et al., 2007). The main area of LIW formation is highlighted by the shaded area. The arrows mark the main intermediate-ocean circulation pathway (Millot and Taupier-Letage, 2005). Both the western and eastern basins are highlighted on the map in different colours and are separated by a red line that indicates the Strait of Sicily, which constitutes the boundary between the two basins. (b) Schematic of the Mediterranean Sea circulation. AW: Atlantic water; MAW: modified Atlantic water; WIW: winter intermediate water; LIW: Levantine intermediate water; WMDM: Western Mediterranean deep water; EMDM: Eastern Mediterranean deep water.

surface waters along the continental shelves of the Gulf of Lion and the Balearic Sea (Figure 1). The intricate relationship between the flow rate of intermediate water and climatic variability in the Mediterranean region makes it an ideal location for investigating the teleconnection between climate and intermediate circulation at the basin scale.

The cross spectral analysis is a tool that helps to identify joint variability between two variables and to assess the phase (lead/lag) between them (e.g. Jevrejeva et al., 2003; Jury et al., 2002; Rigozo et al., 2007). In this study, we quantified for the first time, the phase relationships between the Eastern, central and Western Mediterranean, using both terrestrial (i.e. caves) and marine (i.e. surface and intermediate waters) archives. These phase computations assess periodic leads and lags between records, and highlight climatic/oceanic teleconnections on multi-centennial and millennial time scales over the last 8000 years. We document an out-of-phase relationship between benthic foraminiferal isotope records (both $\delta^{13}C$ and $\delta^{18}O$) and broadly in-phase relationships between the planktonic foraminiferal and spelaeothem isotope records. These findings support the notion of a well-connected atmosphere-surface ocean system that operates largely in tune on millennial timescales throughout the past 8000 years. Furthermore, we infer that the flow rate of the intermediate waters in the western Mediterranean basin (i.e. LIW) were periodically reduced by stronger incursions of Atlantic Water (AW) leading to a partial decoupling from the LIW dynamics in the eastern basin in the past 5000 years.

Oceanographic settings and study sites

Today, the surface Atlantic water (AW) entering the Mediterranean Sea through the Strait of Gibraltar is driven by the combination of dry summers and relatively cold winters, and follows an anti-estuarine circulation. The resulting excess evaporation in the basin causes a steady increase in salinity towards the east of the basin and strongly modifies the AW which quickly becomes the Modified Atlantic Water (MAW, Figure 1). Under this water mass, the LIW, the most voluminous water-mass produced in the Levantine Sea, is flowing (Lascaratos et al., 1993; Millot, 1999; Millot and Taupier-Letage, 2005; Skliris, 2014). The LIW flows westward between 200 and 500 m depth (Figure 1), crossing the Sicily Strait and entering into the Tyrrhenian Sea (Gasparini et al., 2005; Lermusiaux and Robinson, 2001; Millot, 1999) towards the Ligurian Sea and the Gulf of Lion (Millot, 1999).

To utilize cross-spectral analyses effectively, it is necessary to compare geochemical records that respond to the same processes. Therefore, to examine the potential east-west phase relationship of LIW dynamics, we specifically chose marine proxy records that meet the following criteria: (*i*) well dated marine archives located at water depths along the LIW trajectory, with readily available geochemical records from the middle to late Holocene known to capture LIW properties (i.e. temperature, flow rate), (*ii*) marine archives with similar depositional settings and (*iii*) a sufficiently high sedimentation rate during the Holocene to capture periodicities at the centennial and millennial scales. Various approaches have been employed in studies investigating the dynamics of intermediate circulation in the Mediterranean Sea. These include the analysis of foraminiferal ecology, grain size, Nd isotopes, and benthic $\delta^{13}C$ (e.g. Angue Minto'o et al., 2015; Colin et al., 2021; Duhamel et al., 2020; Fach et al., 2021; Hennekam et al., 2014; Incarbona and Sprovieri, 2020; Le Houedec et al., 2020; Rohling et al., 2015; Toucanne et al., 2012). Nevertheless, amongst the existing records, only few possess both comparable depositional settings and comparable geochemical records (in terms of resolution and proxy interpretation). Furthermore, as an pioneer exploration of the East-West phase relationship of LIW during the Holocene, we specifically searched for sites located at the two extremes of the LIW path (the Levantine and Ligurian/Gulf of Lion basins) as well as one site positioned in the middle of the LIW pathway. We selected three marine sediment cores: (i) KESC9-14 in the western Mediterranean from the Ligurian Sea (43.31°N, 7.11°E, Le Houedec et al., 2021), (ii) PS009PC (32°07.7′N, 34°24.4′E, Hennekam et al., 2014; Le Houedec et al., 2020) in the eastern Mediterranean, from the Levantine Sea and (iii) ODP Site 963 (Hole D) (37°02.148′N, 13°10.686′E, Incarbona and Sprovieri, 2020) in the central Mediterranean, close to Sicily Strait (Figure 1). The three cores are located at similar water depths, respectively at 537, 552, and 469 m below sea level, and are positioned on the LIW trajectory. Most importantly, these three cores produced a benthic foraminiferal $\delta^{13}C$ records that was shown to trace the activity of the LIW over the Holocene. The eastern and western cores were analysed for the $\delta^{13}C$ and $\delta^{18}O$ ratios of benthic and planktonic foraminiferal calcite, at comparable time resolutions. This resulted in resolutions of 130 and 80 years (on average) for the benthic records, and 75 and 38 years for the planktonic records, for western site KESC9-14 and eastern site PS009PC, respectively. The central site was analysed for benthic $\delta^{13}C$ and $\delta^{18}O$ records which have comparable time resolutions to the two other cores (around 98 years).

In addition to the marine proxy records, we selected two well-known cave spelaeothem records that border the eastern and western basins, to assess the atmospheric component of potential East-West teleconnections. These records were already extensively studied and were shown to be comparable for periodicity analysis (Zanchetta et al., 2014) and to be representative of the regional climate of their respective areas: Soreq Cave for the East Mediterranean Levantine region (Bar-Matthews et al., 1999, 2003; Bar-Matthews and Ayalon, 2011) and Corchia Cave for the Western Mediterranean Ligurian region (Regattieri et al., 2019; Zanchetta et al., 2007, 2011).

Methods

Age models

We recomputed all ages using 'R' software (Bchron package; R Core Team, 2020) using the calibration curve 'Marine20' (Reimer et al., 2023), mainly because (*i*) the age models of the three marine sediment cores were initially built using different software packages and calibration curves (Hennekam et al., 2014; Incarbona and Sprovieri, 2020; Le Houedec et al., 2021) and (*ii*) to obtain precise and accurate age control, which is needed to obtain meaningful phase computations. For the computation a reservoir age of 400 ± 50 years obtained from the Global Marine Reservoir Database using the average of the nearest reservoir ages (http://calib.org/marine/) was applied. An additional local reservoir correction (ΔR) of 21 ± 63 years was incorporated in the age model of Site PS009PC as suggested in Hennekam et al. (2014). This correction was based on ^{14}C analyses of recent shell material near the core locality (Reimer and McCormac, 2002). New recomputed age models are presented in Figure 2 (data available in the Supplemental Materials). Chronological differences between the Corchia and Soreq Cave isotopic records were previously investigated and found to fall within the uncertainty of each site's individual age-model (Zanchetta et al., 2014). We infer that the $\delta^{18}O$ records of both caves can be analysed for phase relationships using the published age models without further adjustment for the middle to late Holocene (Bar-Matthews and Ayalon, 2011; Zanchetta et al., 2007).

Resampling strategy and time series analysis

For the western Mediterranean core KESC9-14, benthic and planktonic stable carbon ($\delta^{13}C$) and oxygen ($\delta^{18}O$) isotopes were measured at an average resolution of 10 and ~5 cm, respectively (Le Houedec et al., 2021). This corresponds to a resolution of ~100 to ~250 years for the Late-Holocene and middle Holocene time intervals, respectively. For the eastern Mediterranean core PS009PC records, benthic and planktonic foraminiferal isotope records have a sampling resolution of ~150 years for the studied time period (Hennekam et al., 2014; Le Houedec et al., 2020) For the central Mediterranean Site ODP 963D, the planktonic and benthic foraminiferal sampling resolution range from 80 to 100 years on average respectively for the Late-Holocene and Mid-Holocene time intervals (Incarbona and Sprovieri, 2020). To avoid aliasing effects, only periodicities >800 years will be discussed here. Prior to frequency and phase-computations, we linearly interpolated records at a step average of 75 years for the planktonic records, 150 years for the benthic records and 50 years for the cave records (Supplemental Materials).

Frequency spectrum analysis (Figures 3–5) were performed on the linearly interpolated records using RedFit spectral analysis on PAST 4.03 software (Hammer et al., 2001). Frequencies are significant when above the null hypothesis (Monte Carlo).

Time-averaged (i.e. from 8–0 ka) phase computations were performed using Blackman-Tukey cross-spectral analyses (BT) calculations with the software programme Analyseries (Paillard et al., 1996). Phase relationships are only depicted when frequencies are coherent above the 80% and 95% confidence levels (shaded and full

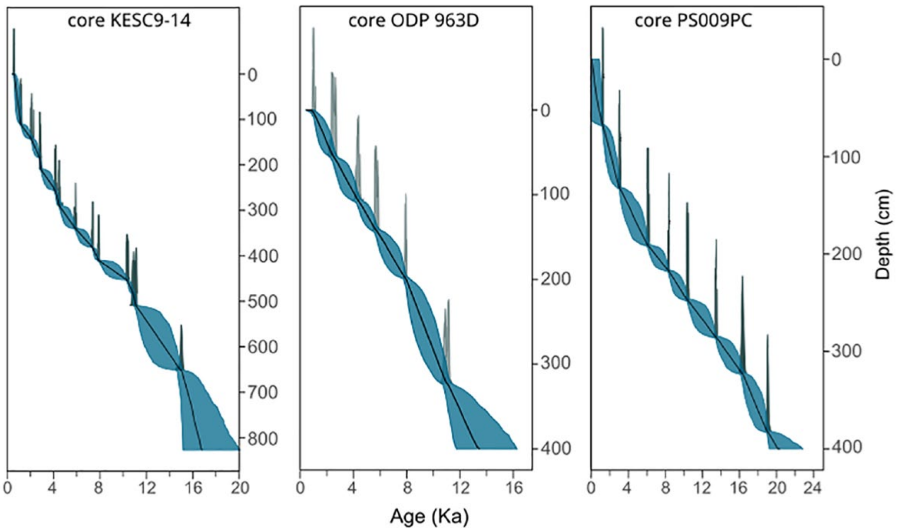

Figure 2. Age models of marine cores KESC9-14 (Ligurian Basin), ODP 963D (Sicily Strait) and PS009PC (Levantine Basin). Age models were calculated using Marine20 curve in Bchron R package (R Core Team, 2020).

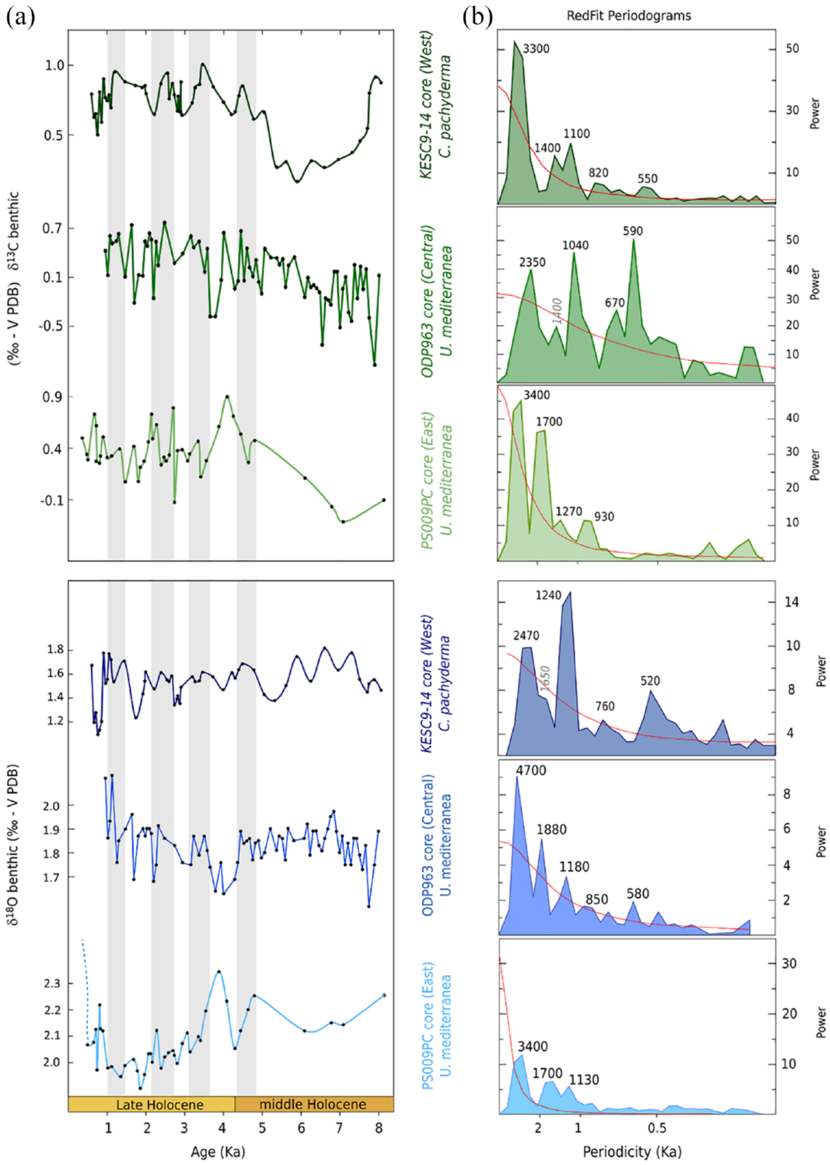

Figure 3. Benthic foraminiferal $\delta^{13}C$ and $\delta^{18}O$ records from the western (Core KESC9-14), central (Site ODP 963), and eastern (Core PS009PC) sites. (a) Benthic foraminiferal stable isotopic records from the three cores. The shaded areas highlight the intervals in which the records appear visually to be variable on millennial time scales (b) RedFit periodograms of the records. The red line represents the null hypothesis (red noise model) above which the periodicities are significant. The main periodicities of the benthic records are indicated.

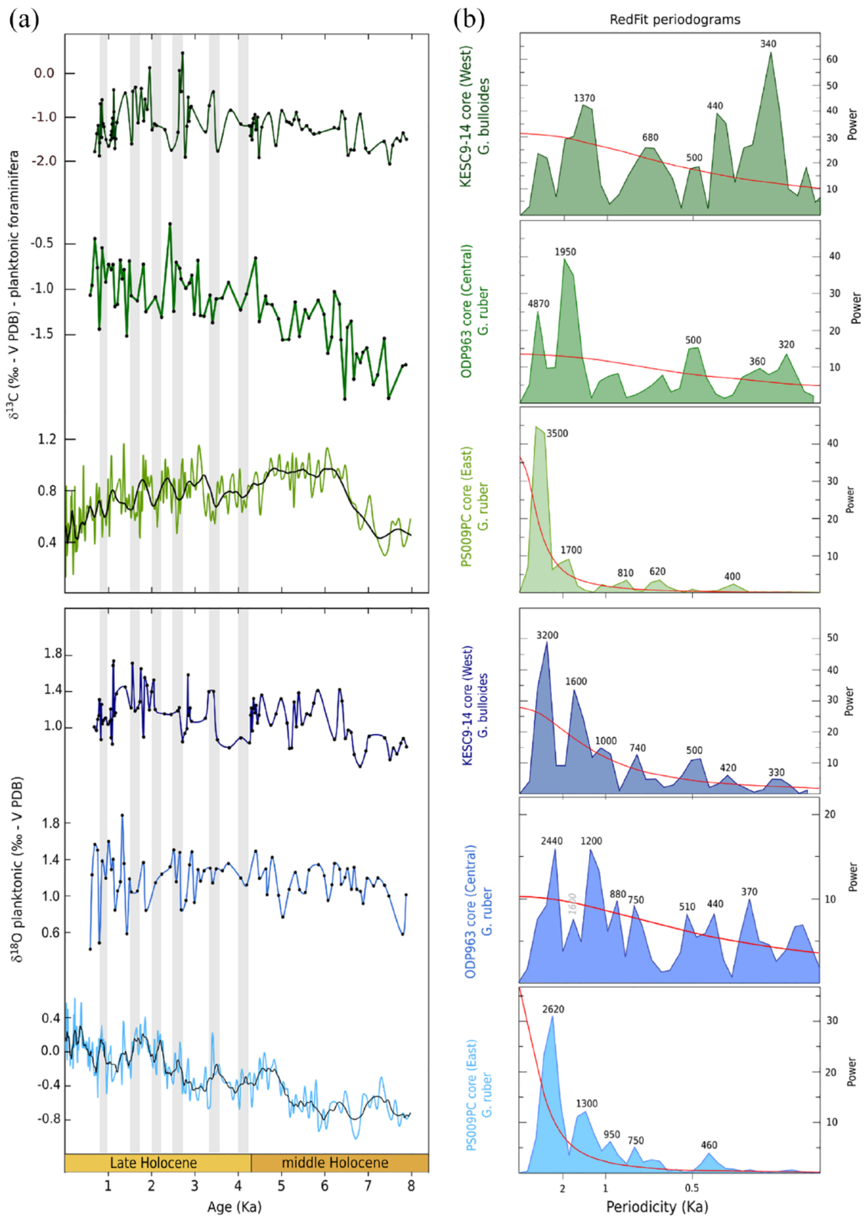

Figure 4. Planktonic foraminiferal $\delta^{13}C$ and $\delta^{18}O$ records from the western (Core KESC9-14), central (Site ODP 963), and eastern (Core PS009PC) cores. (a) Planktonic foraminiferal ^{TM13}C and ^{TM18}O records from both cores. The black lines are the 5-point moving averages, used for the computations of the RedFit periodograms. The shaded areas highlight the intervals in which the records appear visually to be variable on millennial time scales. (b) RedFit periodograms of the records. The main periodicities of the planktonic records are indicated. The red line represents the red noise null hypothesis above which the periodicities are significant.

colours, respectively, see Figures 6–10). In addition, time-evolutive phase coherence and phase-relationships between eastern and western archives was investigated through wavelet coherence (WC) computed on R software (R Core Team, 2020) using the 'Biwavelet package' (Gouhier et al., 2018). The WC computation reveals areas of high common power scaled with r^2 significance, which is estimated using the Monte Carlo method. Evolutive phase relationships above 95% level of confidence are shown as arrows that are superimposed on the phase coherence plots. In-phase relationships are indicated by arrows that are pointing to the right, and anti-phase relationships by arrows that are pointing to the left. Upward (downward) pointing arrows indicate that the second (first) variable leads the first (second) variable by $\Pi/2$.

Results

RedFit spectral analysis

The main periodicities observed in the planktonic and benthic $\delta^{18}O$ and $\delta^{13}C$ records from the three marine sites are around 900–1100 years (Figures 3 and 4), in agreement with what has been previously published on these records (Hennekam et al., 2014; Incarbona and Sprovieri, 2020; Le Houedec et al., 2020, 2021; Mojtahid et al., 2015). A secondary concentration of spectral power is observed in the periodicity range between 1400 and 1800 years, which is present in both the planktonic and benthic $\delta^{18}O$ and $\delta^{13}C$ records from the three sites. Power spectral results of the cave data (Figure 5) reveal that the main centennial and millennial periodicities observed in the benthic and planktonic $\delta^{18}O$ and $\delta^{13}C$ records are also expressed in the spelaeothem $\delta^{18}O$ records.

Coherency and phase relationships between benthic foraminiferal isotope records

Wavelet coherence (WC) and cross-spectral analyses (calculated in the frequency domain) are robust against small-to-modest changes in the age model (up to 160 years, supplemental data, i.e. changes in the time domain). The Blackman-Tukey cross-spectral

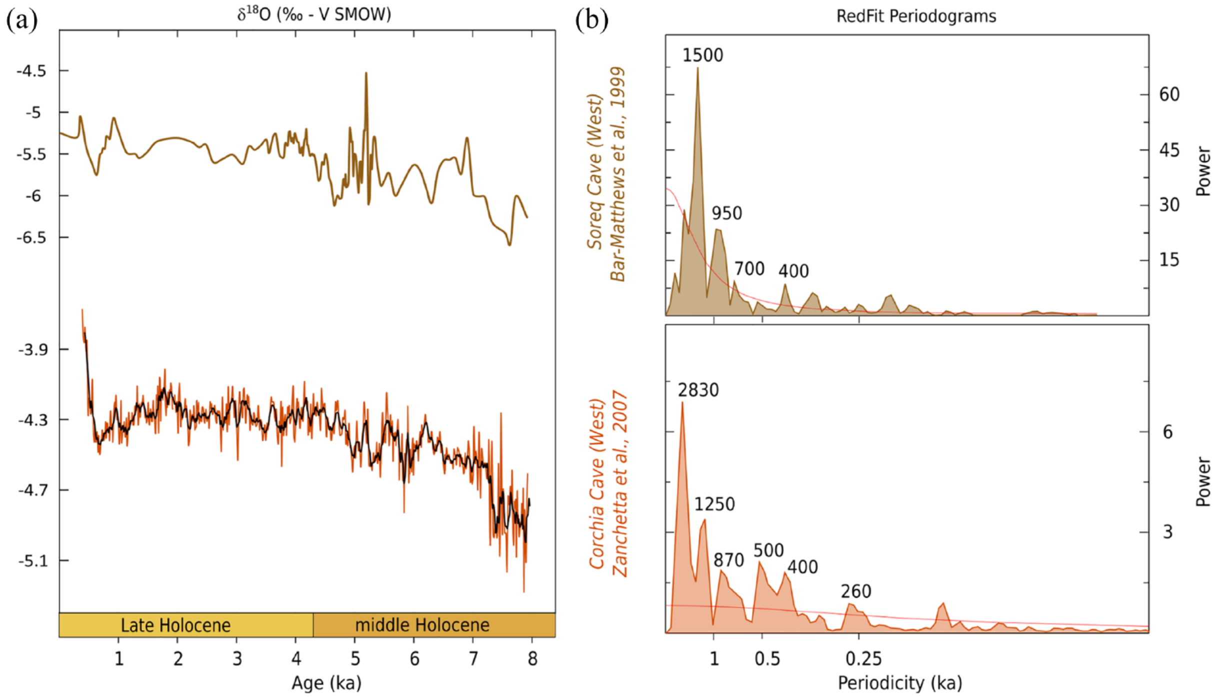

Figure 5. $\delta^{18}O$ spelaeothem records from the Soreq (Bar-Matthews et al., 1999) and Corchia (Zanchetta et al., 2007) caves. (a) $\delta^{18}O$ records from both caves. The black lines are the 5-point moving averages, used for the computations of the RedFit periodograms. (b) RedFit periodograms of the records. The main periodicities of the records are indicated. The red line represents the red noise null hypothesis above which the periodicities are significant.

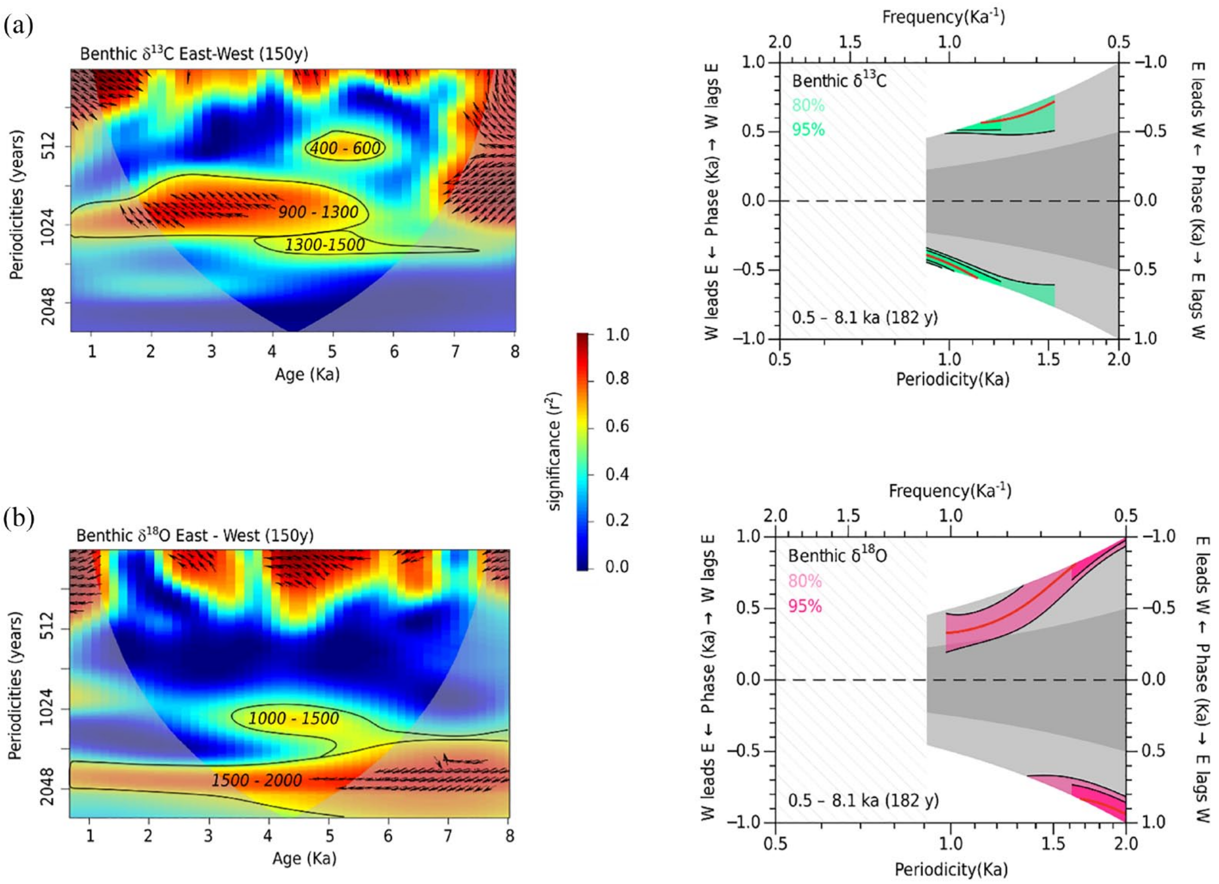

Figure 6. Coherency and phase computations between the benthic foraminiferal $\delta^{13}C$ and $\delta^{18}O$ records from the western (Core KESC9-14) and eastern (Core PS009PC) Mediterranean basins. (a) Phase analyses on benthic $\delta^{13}C$ records. (b) Phase analyses on benthic $\delta^{18}O$ records. Wavelet coherence (WC) is presented on the left side of the panel. WC resampling resolution is given between brackets. The colour indicates the significance of the coherence of periodic signals found in both records. The black line was set to $r^2 = 0.60$. Superimposed phase-arrows are presented above 95% level of confidence, that point to the right (left) when periodicities are in phase (anti-phase), and arrows are pointing to the up (down) when the second (first) variable is leading by $\Pi/2$. Blackman-Tukey phase computations (BT) are presented on the right of the panel. Shaded colours indicate the 80% confidence level on error bars, full colours the 95% level. The age range indicates the time window over which the average phase relationship was computed, with the accompanying resampling resolution given in between brackets.

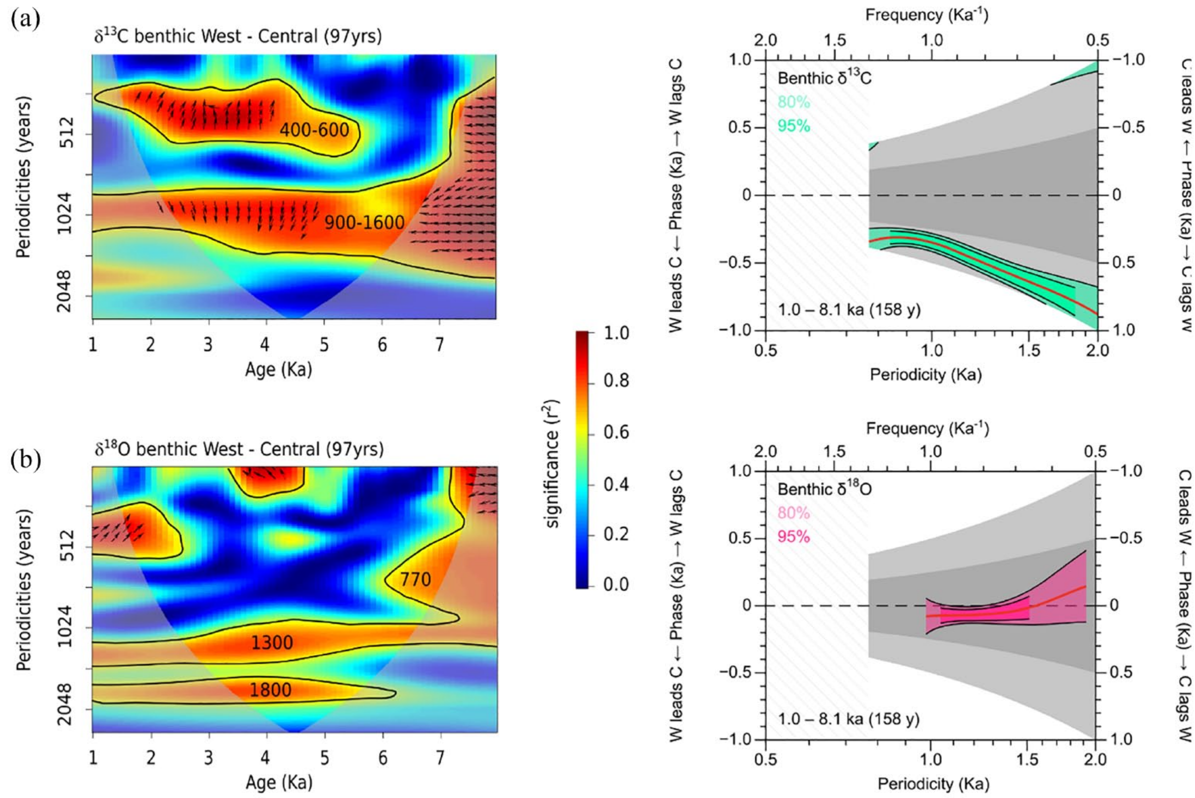

Figure 7. Coherency and phase computations between the benthic foraminiferal $\delta^{13}C$ (panel a) and $\delta^{18}O$ (panel b) records of central (ODP 963D) and western (KESC9-14) cores. See Figure 6 for the detailed legend of WC (left panels) and BT (right panels) computations.

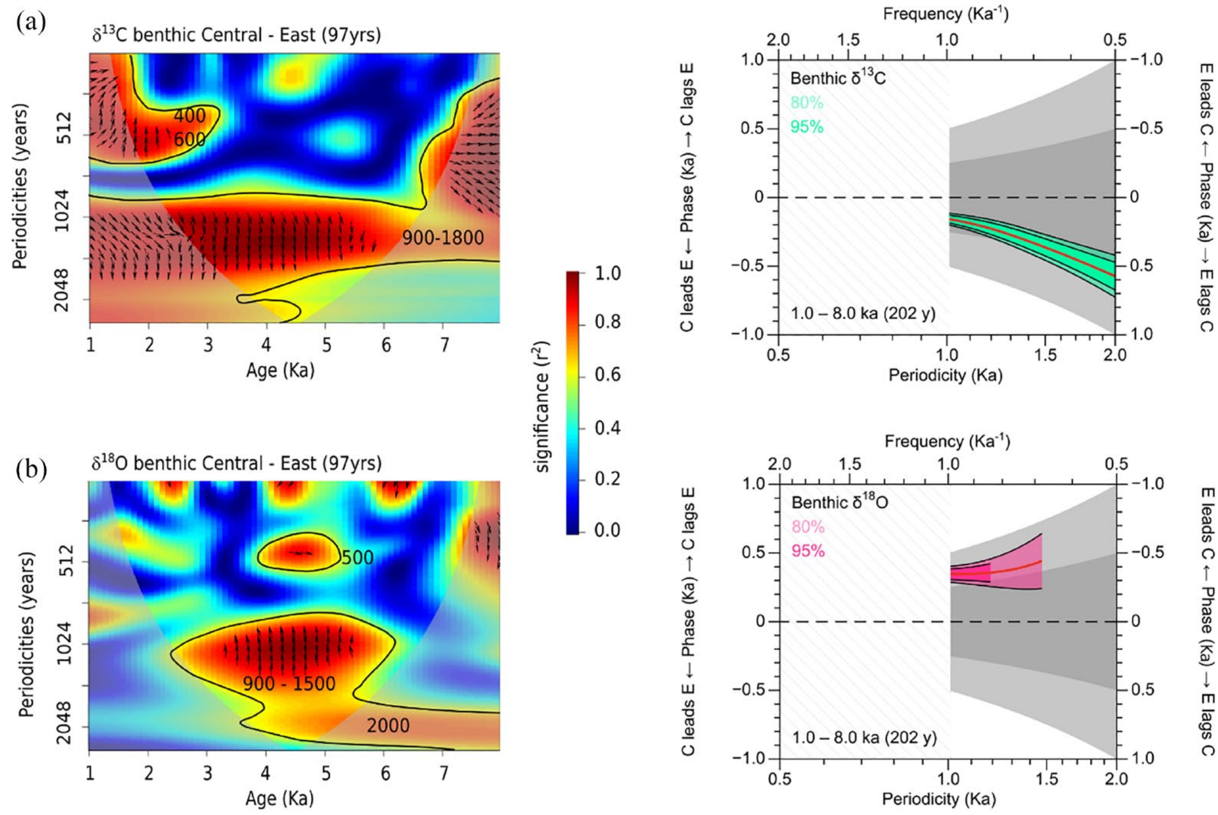

Figure 8. Coherency and phase computations between the benthic foraminiferal $\delta^{13}C$ (panel a) and $\delta^{18}O$ (panel b) records of central (ODP 963D) and eastern (PS009PC) cores. See Figure 6 for the detailed legend of WC (left panels) and BT (right panels) computations.

analyses exclusively involve phase calculations that are appropriate for the resampling resolutions of the utilized records. No computations are conducted for centennial periodicities below 500 years, as they are not adequately resolved.

The $\delta^{13}C$ records. Wavelet coherence (WC) calculations on the eastern and western benthic foraminiferal $\delta^{13}C$ records show a highly significant coherency for the 900–1300 year periodicities over the last 5 kyrs ($r^2 > 0.70$) (Figure 5a). From this

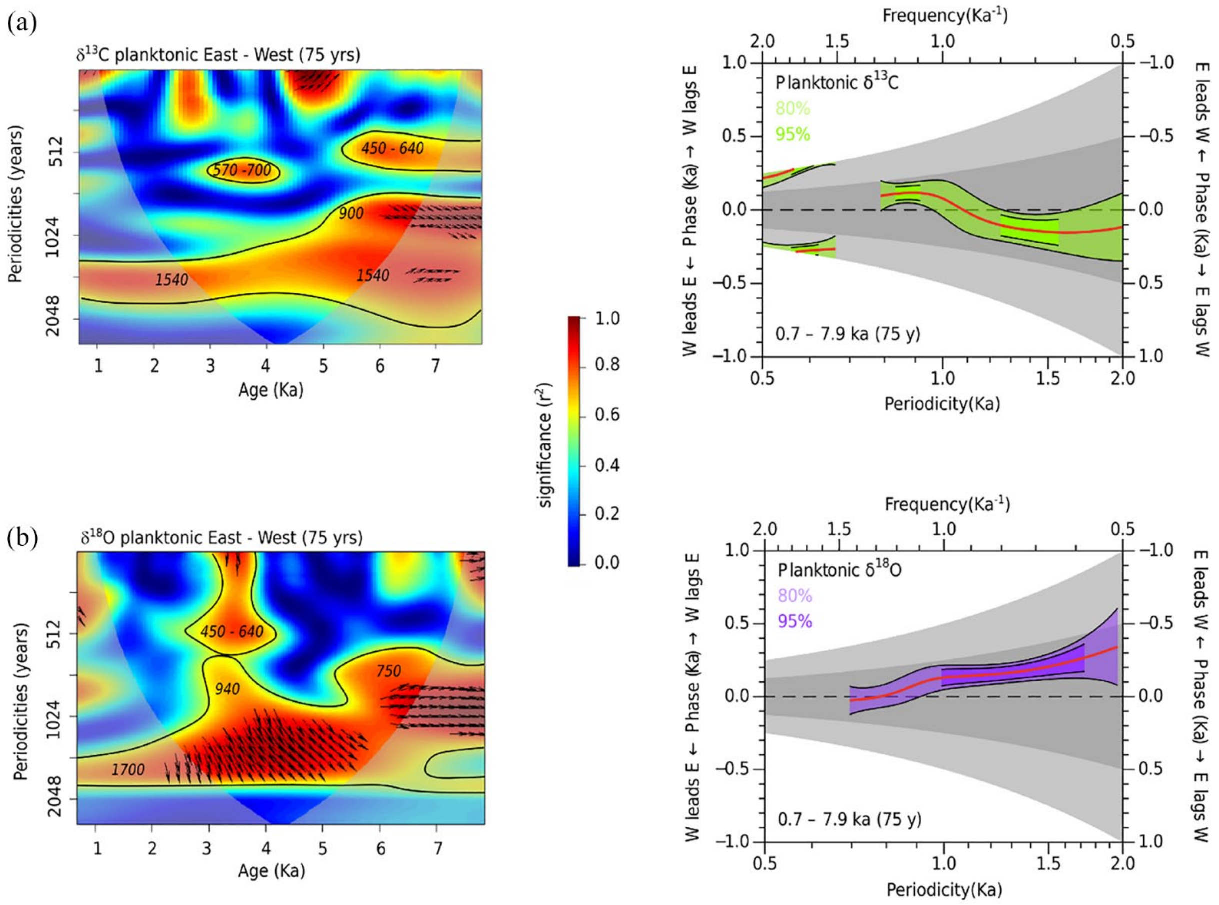

Figure 9. Coherency and phase computations for the planktonic foraminiferal $\delta^{13}C$ (panel a) and $\delta^{18}O$ (panel b) records from eastern (Core PS009PC) and western (Core KESC9-14) basins. See Figure 6 for the detailed legend of WC (left panels) and BT (right panels) computations.

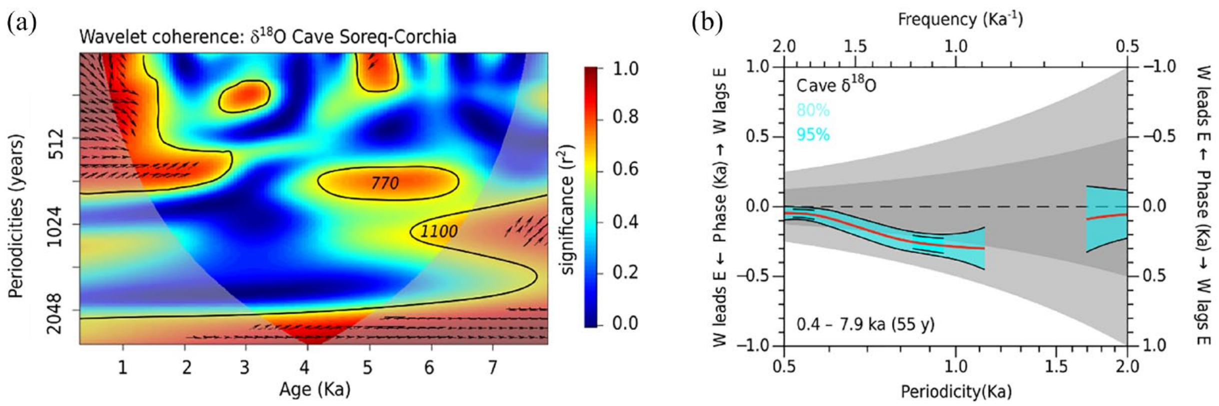

Figure 10. Coherency and phase computations between spelaeothem $\delta^{18}O$ records from the Soreq and Corchia caves. (a) Wavelet coherence analysis. (b) BT Time-averaged phase relationship between eastern (Soreq Cave) and western (Corchia cave) $\delta^{18}O$ records. See Figure 6 for the detailed legend of WC (left panels) and BT (right panels) computations.

computation, an anti-phase relationship with high significance is expressed for the 900–1300 year periodicities (confidence level = 95%). Furthermore, we find a coherence of periodicity around 1400 years over the 4–8 kyrs time interval, but with lower significance ($r^2 = 0.65$). Averaged over the 8–0 ka time interval, similar anti-phase results are found with the Blackman-Tukey (BT) phase computations. Furthermore, although with lower significance, but still above = 80% confidence level, the BT phase computation shows that an anti-phase relationship also exists between the eastern and western benthic foraminiferal $\delta^{13}C$ records for the higher 1400–1600 years periodicities. Between the central and the western benthic foraminiferal $\delta^{13}C$ records, the coherency is highly significant for the 900–1600 year periodicities, and both the WC and BT computation display an almost completely anti-phase relationship for this range of periodicities (Figure 6a). Between 5.5 and 1 ka the WC reveals coherence at the 400–600 year periodicity, which is also marked by a near out-of-phase relationship. The results from WC obtained between the central and eastern $\delta^{13}C$ records indicate high coherency for periodicities between 900 and 1800 years (Figure 7a). Both WC and BT results indicate that the central benthic foraminiferal $\delta^{13}C$ record from Site 963 lead the western benthic foraminiferal $\delta^{13}C$ record of the PS009PC core by a quarter of cycles on all periodicities between 1000 and 2000 years.

The δ^18^O records. The WC analysis performed on the benthic foraminiferal $\delta^{18}O$ records from both eastern and western cores (Figure 5b) is highly significant ($r^2 > 0.85$) for the 1500–2000 year periodicities across the entire 8–0 ka time interval. In addition, a significant coherency ($r^2 = 0.60$) for the 1000–1500 year periodicities is present for the time interval between 6 and 3 ka between the benthic foraminiferal $\delta^{18}O$ record. From the WC analyses, we find an anti-phase relationship between benthic foraminiferal $\delta^{18}O$ records from East and West on the 1500–2000 year periodicities. The time-averaged BT phase computations support these findings and highlight further anti-phase relationships down to 1000 years periodicities, albeit with less significance. The benthic foraminiferal $\delta^{18}O$ record of the western and central cores show strong coherency for periodicities around 1300 and 1800 years (Figure 6b). From the WC computation, we derive that the records are in-phase for those periodicities. The WC results are confirmed by the BT computations that show a fully in-phase relationship between the benthic foraminiferal $\delta^{18}O$ records from both sites for the 1000–2000 year periodicities. Between the central and eastern benthic foraminiferal $\delta^{18}O$ records (Figure 7b), we find that the $\delta^{18}O$ record of the eastern core (PS009PC) leads by a quarter of cycles the $\delta^{18}O$ record of the central site (Site 963) on periodicities ranging between 1000 and 1500 years.

Coherency and phase relationships between planktonic foraminiferal isotope records

For both the planktonic foraminiferal $\delta^{13}C$ and $\delta^{18}O$ records (Figure 8a), the 900–1000 year periodicity is in coherence of phase from 8 to 4.5 ka, while the 1500–1700 frequencies are highly coherent between the eastern and western records ($r^2 > 0.80$) over all the studied time interval. A clear in-phase relationship was found between the two $\delta^{13}C$ records and an almost in-phase relationship (i.e. about one-eighth of cycle delay of the western record) was found between the two $\delta^{18}O$ records for all periodicities between 800 and 1700 years. These results are broadly supported by the time-averaged BT cross-spectral analysis (Figure 8b).

Coherency and phase relationships between cave oxygen isotope records

The coherence and phase analyses (Figure 8a) between both eastern and western caves indicates a strong correlation for periodicities <800 years, and at around 1100 years between 8 and 5 ka. WC analysis does not show a clear phase relationship (Figure 9a). However, from the BT computation (Figure 9b) we observe a lead of a quarter of cycle of the western record at the periodicities from 800 to 1100 years. Both analyses show a lack of coherency on the periodicities ranging from 1200 to 1800 years periodicities.

Discussion

Proxy record significance for phase computations

To investigate atmospheric and oceanic teleconnections between the eastern and western Mediterranean basins during the Holocene, it is necessary to make sure that the proxies used respond to similar processes (e.g. temperature, runoff, circulation). The most recent publications on the three marine sediment records interpret the benthic foraminiferal $\delta^{13}C$ signal as reflecting LIW ventilation (i.e. flow rate) with little/no effect of productivity and organic matter flux to the seafloor, and the $\delta^{18}O$ as a proxy for bottom water temperature/$\delta^{18}O$ signature of the sea water (Incarbona and Sprovieri, 2020; Le Houedec et al., 2020, 2021; Mojtahid et al., 2015). Due to the location of cores KESC9-14 and PS009PC, that is, in front of the Var and Nile river mouths, respectively, their planktonic stable isotopic signals are strongly influenced by the fluvial discharge. The planktonic foraminiferal $\delta^{13}C$ signal depends on the dissolved inorganic carbon ($\delta^{13}C$-DIC) of surface waters, which in the two studied regions largely depends on continental inputs brought by the local rivers and thus on the regional hydroclimate (Hennekam et al., 2014; Le Houedec et al., 2020; Mojtahid et al., 2015).

Planktonic foraminiferal $\delta^{18}O$ from the eastern site PS009PC likely reflects the Nile activity and therefore precipitation on the African continent (Hennekam et al., 2014; Le Houedec et al., 2020). Similarly, the planktonic foraminiferal $\delta^{18}O$ record from the western site KESC9-14 appears to be modulated by the activity of the Var river system that responds to the European hydroclimate (Le Houedec et al., 2021). As such, those two planktonic $\delta^{18}O$ records are respectively tracking the two primary climatic influences on the Mediterranean Sea, one from the warm climatic domain of Africa, and the other one from the mild climate domain of mid-latitude Europe. Therefore, the planktonic $\delta^{13}C$ and $\delta^{18}O$ records from the eastern and western sediment cores are well-suited for investigating potential lead-lag and/or phase relationships between the large-scale atmospheric (precipitation) changes of the two regions. The central marine Site 963, however, is located in open marine waters and the planktonic foraminiferal $\delta^{13}C$ and $\delta^{18}O$ records from this site are interpreted as indicators of surface ocean primary production and sea surface temperatures, respectively (Incarbona and Sprovieri, 2020). As such, the process driving the planktonic stable isotopic variability at Site 963 is too different from those driving the variability of the two other cores, and therefore these proxies were not used for phase computations. Lastly, the $\delta^{18}O$ records from both the Corchia (western region) and Soreq (eastern region) caves are reliable proxies for regional precipitation (Bar-Matthews et al., 1999; Regattieri et al., 2019), thereby again reflecting regional climatic conditions.

East-west ocean-atmosphere teleconnections in the Mediterranean

Millennial scale in-phase atmospheric teleconnection. Our findings from the cave $\delta^{18}O$ results based on the WC and BT phase computations (Figure 10) agree with previous findings (Zanchetta et al., 2014) based on data peak correlations. Zanchetta et al. (2014) described: (*i*) coeval multi-centennial climatic events between Soreq and Corchia $\delta^{18}O$ records for the 6–4 ka intervals for which we report an in-phase relationship (<800 years) and (*ii*) a lack of agreement between 7 and 6 ka, which likely corresponds to the ~¼ lead of the western cave for the 700–1100 year periodicities in our BT phase analysis (Figure 10). The absence of correlation between the two cave $\delta^{18}O$ records between 7 and 6 ka has been interpreted to be the result of a decrease in the effective moisture in the Soreq region (Zanchetta et al., 2014). Alternatively, the ~¼ cycle lead of the western cave $\delta^{18}O$ record with respect to the eastern one, may suggest that hydroclimatic changes on multi-centennial time scales between 7 and 6 ka initiated in the West and gradually moved eastward, thereby revealing perhaps an Atlantic influence on atmospheric rainfall patterns during this specific period. Anyway, and because the ~¼ lead of the western cave is found during a short period of the middle to late Holocene, we consider that both eastern and western cave records coeval climatic oscillation which are broadly in-phase for the 900–1700 years periodicities. This suggests that hydroclimate conditions between the eastern and western circum Mediterranean regions were relatively closely coupled on multi-centennial to millennial timescales for the last ~8 ka as already suggested by Zanchetta et al. (2014). The planktonic records are in agreement with the cave records by showing a broadly in-phase relationship on multi-centennial to millennial time scales between eastern and western sites for all periodicities from 900 to 1700 years, albeit with small deviations from a perfect in-phase relationship. From the eastern Mediterranean planktonic stable isotopic records, the 500–1000 year periodicities during the early to middle Holocene have been interpreted to reflect the solar-forced variability in North African monsoon strength (Hennekam et al., 2014). Similarly, the planktonic stable isotopic records of the western Mediterranean Site KESC9-14 were interpreted as the solar-forced variability of the precipitation regime in Europe (Le Houedec et al., 2021). Periodicities ranging between 1300 and 1800 years documented in the planktonic foraminiferal $\delta^{18}O$ and $\delta^{13}C$ records from Sites PS009PC and KESC9-14 is a feature widely observed in geochemical records from the Atlantic Ocean (Bianchi and McCave, 1999; Bond et al., 1997; Campbell et al., 1998; O'Brien et al., 1995; Sirocko et al., 1996). For the Holocene, this range of periodicities in the Atlantic Ocean has been linked to internal forcing (i.e. variability of the north Atlantic oceanic circulation, Broecker et al., 1999; Debret et al., 2007; McManus et al., 1999). It is interesting to note that, at this range of periodicities, there is no phase relationship between the cave records (Figure 10). This seems to support the hypothesis of an oceanic origin for the 1300–1800 years cyclicity. Conversely, we interpret the (near) in-phase signal in both planktonic and cave records within periodicities between 900 and 2000 years, as evidence of a well-mixed and interconnected atmospheric system between the two Levantine and Ligurian regions of the Mediterranean with no substantial lead or lags were able to establish. While there is evidence for local climatic modulation across the Mediterranean Sea at shorter timescales (e.g. Ait Brahim et al., 2018; Conte et al., 1989; Di Rita et al., 2018; Dormoy et al., 2009; Jalut et al., 2000; Magny et al., 2013; Peyron et al., 2011), our findings indicate that, within this range of periodicities, the surface hydro-climatic evolution between the Levantine and Ligurian basins was closely linked on multi-centennial to millennial time scales over the last 8 kyrs.

Millennial scale anti-phase oceanic teleconnection. In stark contrast to the planktonic and cave records, we observe distinct out-of-phase relationships between both benthic foraminiferal $\delta^{13}C$ records from the eastern and western sites, and from the central and western sites (Figures 6 and 7) for the 1000–2000 years periodicities. Because the benthic $\delta^{13}C$ record from these three sites is thought to reflect the flow strength of the LIW, this would mean that the central Site 963 is under the same LIW influence as the eastern site. This interpretation is supported by the phase-relationship between benthic foraminiferal $\delta^{13}C$ records from the eastern and central sites, that are closer to an in-phase relationship than to being out of phase. In short: millennial LIW dynamics at Site 963 record predominantly an East Mediterranean oceanographic signal. Furthermore, our data indicate that the LIW flow rate intensity is modulated differently for periodicities ranging from 1000 to 2000 years between the central-east and west Mediterranean basins (i.e. weak/strong intensity in the central-east/west correspond to strong/weak intensity in the west/central-east, respectively). These out-of-phase signals cannot be explained by the effect of the time needed for the LIW to bring a signal from the eastern to the western basin because the overturning Mediterranean circulation is ~50 to 100 years (Millot and Taupier-Letage, 2005).

This central-east/west antiphase in the benthic $\delta^{13}C$ records for the 1000–2000 years periodicities occurs in a context of an in-phase atmospheric teleconnection between the eastern and western basins (cf. Section 5.2.1). As such, we invoke from these opposite phase-relationships that the benthic $\delta^{13}C$ records respond primarily to oceanic processes that seem to differ between central/eastern and western basins. In the Mediterranean Sea, MAW and LIW play a central role in the thermohaline circulation contributing to the dense water formation in this enclosed basin (Bethoux, 1980; Bryden et al., 1994; Bryden and Stommel, 1984; Candela, 2001; Tsimplis and Bryden, 2000; Vargas et al., 2006). We hypothesize that the out-of-phase relationships between the two basins at the 1000 and 2000 year periodicities, may relate to an impact of Atlantic Ocean water on intermediate water formation, happening more prominently in the western Mediterranean. The Atlantic Ocean is marked by a millennial mode of variability (i.e. Bond cycles), which is roughly expressed in the periodicity range between 1300 and 1800 years (Bianchi and McCave, 1999; Bond et al., 1997; Campbell et al., 1998; O'Brien et al., 1995; Sirocko et al., 1996) and linked to the north Atlantic oceanic circulation (Broecker et al., 1999; Debret et al., 2007; McManus et al., 1999). The presence of, what we interpret to be, an Atlantic spectral feature (i.e. the ~1500 years periodicity) was previously identified in palaeoclimatic records from the western Mediterranean. An Atlantic influence on the Mediterranean was previously hypothesized as a potential mechanism influencing precipitation rate and storminess events in the Gulf of Lion on millennial timescales (Azuara et al., 2020). In addition, we propose that periodic changes in Atlantic thermohaline circulation on millennial time scales, also impacted the oceanic circulation in the Mediterranean and affected the strength and/or production rate of the Western Intermediate Water (WIW) in the western basin. Indeed, although the main branch of the MAW flows along the southern Mediterranean margin and through the strait of Sicily, a small branch of the MAW has an anti-clockwise circuit along the coastline of the western basin and bathes the Ligurian Sea (Millot, 1999). Argo float data revealed that in the Ligurian Sea, WIW, LIW and MAW water masses are hardly distinguishable, in terms of temperature and salinity, due to vertical mixing (Fedele et al., 2022). In the present-day western basin, the WIW is seasonally produced under the effect of cool north westerly winds in the Gulf of Lion and Balearic Sea (Juza et al., 2013, 2019; Petrenko, 2003; Salat and Font, 1987). Therefore, we suggest that the transport of less saline waters, such as MAW, might change the depth of pycnocline and affect the WIW production rate as well as the LIW incursion into the western Mediterranean basin.

The clear out-of-phase relationship obtained from benthic $\delta^{18}O$ records between eastern and western sites is in agreement with benthic $\delta^{13}C$ for the periodicities ranging from 1000 to 2000 years (Figure 6). This means that, in addition to an east-west modification of the LIW flow rate, we also modify the physical parameters (i.e. temperature, salinity) of the water mass. This supports the cyclic contribution of the MAW flow into the western Mediterranean basin, which influences the temperature/salinity of both the WIW and LIW due to regional mixing (Figure 1). Flowing eastward, the MAW is highly modified in terms of salinity and temperature (e.g. Pinardi et al., 2019; Theocharis et al., 2002; Vargas-Yanez et al., 2017; Wüst, 1961), the strait of Sicily reduces its west-east flux, and the more regional origin the LIW formation, minimize the direct influence of the Atlantic water masses in this basin. One could argue that such changes in surface water properties (temperature/salinity) under the influence of MAW must be recorded in the planktonic $\delta^{18}O$. However, due to the proximity of our eastern and western sites to major river systems, we think that the seawater isotopic signature was overprinted by the river inputs. The benthic foraminiferal $\delta^{18}O$ phase results obtained with the central site ODP 963D appear to be largely in phase with the western site while it is in one-fourth of cycle out of phase with the eastern site. This recorded signal may be due to the intermediate geographical position of site ODP 963D leading to an 'in between' temperature and salinity properties of the flowing water mass.

Conclusions

In this study, we assemble terrestrial and marine climate stable isotopic proxy records on which we applied cross-spectral analysis to investigate the atmospheric and oceanic teleconnections between the eastern, central and western Mediterranean. We find that the atmosphere and surface ocean are well coupled and marked by climate records (temperature, precipitation) that show similar variability. Furthermore, this variability is found to be largely in-phase on multi-centennial to millennial time scales between the Levantine and the Ligurian regions over the last 8 kyrs.

In stark contrast, we find that Levantine intermediate waters flow rate is marked by a distinct out-of-phase relationship between the eastern/central and western Mediterranean for the 1000–2000 year periodicities. We speculate that this see-saw pattern reflects the intrusion of Atlantic Water into the West Mediterranean modulating the rate of formation of the WIW in the western basin. Differential mixing of WIW/LIW with MAW at centennial and millennial time scales in the Western Mediterranean may highlight the expression of similar cycles found in the Atlantic region. At the same time, in the eastern basin the LIW remained under persistent regional climatic/oceanographic influence.

We assess, for the first time, phase relationships on multi-centennial and millennial time scales (i.e. Mid to Late-Holocene) and show that phase computations can be used successfully to investigate East-West atmospheric and oceanic teleconnections in the Mediterranean Sea. We emphasize that the main limitation of using such technique reside in the availability of comparable datasets (depositional setting, depth, proxy used and its significance and time resolution) between the studied areas. To further investigate intermediate to deep water circulation patterns between the eastern and western Mediterranean, we suggest following up with studies using other geochemical proxies (e.g. Neodymium isotopes) for both regions, and generating better resolved time series.

Acknowledgements

We thank the editor and two reviewers for support and suggestions.

Funding

The author(s) disclosed receipt of the following financial support for the research, authorship, and/or publication of this article: This study was carried out in the context of collaboration between the University of Geneva (under funding no. S18173, PI: Elias Samankassou), the National Oceanography Centre in Southampton, The University of Manchester, the NIOZ, and the University of Angers (TANDEM project funded by France's Regional Council of Pays de la Loire).

ORCID iD

Sandrine Le Houedec https://orcid.org/0000-0002-4938-5613

Supplementary material

Supplementary Material (data tables of recomputed age model and interpolated stable isotopic data set used for the computation) can be found on the Mendeley data repository (https://data.mendeley.com/datasets/m7whnv4gdf).

References

Ait Brahim Y, Wassenburg JA, Cruz FW et al. (2018) Multi-decadal to centennial hydro-climate variability and linkage to solar forcing in the western Mediterranean during the last 1000 years. *Scientific Reports* 8: 17446.

Angue Minto'o CM, Bassetti MA, Morigi C et al. (2015) Levantine intermediate water hydrodynamic and bottom water ventilation in the northern Tyrrhenian Sea over the past 56,000 years: New insights from benthic foraminifera and ostracods. *Quaternary International: the Journal of the International Union for Quaternary Research* 357: 295–313.

Azuara J, Sabatier P, Lebreton V et al. (2020) Mid- to late-Holocene Mediterranean climate variability: Contribution of multi-proxy and multi-sequence comparison using wavelet spectral analysis in the northwestern Mediterranean basin. *Earth-Science Reviews* 208: 103232.

Bahr A, Kaboth S, Jiménez-Espejo FJ et al. (2015) Persistent monsoonal forcing of Mediterranean outflow water dynamics during the late pleistocene. *Geology* 43: 951–954.

Bar-Matthews M and Ayalon A (2011) Mid-holocene climate variations revealed by high-resolution speleothem records from Soreq Cave, Israel and their correlation with cultural changes. *The Holocene* 21: 163–171.

Bar-Matthews M, Ayalon A, Gilmour M et al. (2003) Sea–land oxygen isotopic relationships from planktonic foraminifera and speleothems in the Eastern Mediterranean region and their implication for paleorainfall during interglacial intervals. *Geochimica et Cosmochimica Acta* 67: 3181–3199.

Bar-Matthews M, Ayalon A, Kaufman A et al. (1999) The eastern Mediterranean paleoclimate as a reflection of regional events: Soreq cave, Israel. *Earth and Planetary Science Letters* 166: 85–95.

Bethoux JP (1980) Mean water fluxes across sections in the Mediterranean Sea, evaluated on the basis of water and salt budgets circulation and of observed salinities. *Oceanologica Acta* 3: 79–88.

Bianchi GG and McCave IN (1999) Holocene periodicity in North Atlantic climate and deep-ocean flow south of Iceland. *Nature* 397: 515–517.

Bond G, Showers W, Cheseby M et al. (1997) A pervasive millennial-scale cycle in North Atlantic holocene and glacial climates. *Science* 278: 1257–1266.

Broecker WS, Sutherland S and Peng TH (1999) A possible 20th-century slowdown of southern ocean deep water formation. *Science* 286: 1132–1135.

Bryden HL, Candela J and Kinder TH (1994) Exchange through the Strait of Gibraltar. *Progress in Oceanography* 33: 201–248.

Bryden HL and Stommel H (1984) Limiting processes that determine basic features of the circulation in the Mediterranean Sea. *Oceanologica Acta* 7: 289–296.

Bye JAT (1996) Coupling ocean — Atmosphere models. *Earth-Science Reviews* 40: 149–162.

Cabos W, de la Vara A, Álvarez-García FJ et al. (2020) Impact of ocean-atmosphere coupling on regional climate: The Iberian Peninsula case. *Climate Dynamics* 54: 4441–4467.

Cacho I, Grimalt JO, Canals M et al. (2001) Variability of the western Mediterranean sea surface temperature during the last 25,000 years and its connection with the Northern Hemisphere climatic changes. *Paleoceanography* 16: 40–52.

Cacho I, Grimalt JO, Pelejero C et al. (1999) Dansgaard-Oeschger and Heinrich event imprints in Alboran Sea paleotemperatures. *Paleoceanography* 14: 698–705.

Cacho I, Grimalt JO, Sierro FJ et al. (2000) Evidence for enhanced Mediterranean thermohaline circulation during rapid climatic coolings. *Earth and Planetary Science Letters* 183: 417–429.

Campbell ID, Campbell C, Apps MJ et al. (1998) Late Holocene ~1500 yr climatic periodicities and their implications. *Geology* 26: 471–473.

Candela J (2001) Chapter 5.7 Mediterranean water and global circulation. In: Siedler G, Church J and Gould J (eds) *International Geophysics, Ocean Circulation and Climate*. Cambridge: Academic Press, pp.419–XLVIII.

Christensen JH, Kanikicharla KK, Aldrian E et al. (2013) Climate phenomena and their relevance for future regional climate change. In: Stocker TF, Qin GKP, Tignor M, et al. (eds) *Climate Change 2013. The Physical Science Basis: Working Group I Contribution to the Fifth Assessment Report of the Intergovernmental Panel on Climate Change*. Cambridge, UK, New York, NY, USA: Cambridge University Press, pp.1217–1308.

Clark PU, Shakun JD, Marcott SA et al. (2016) Consequences of twenty-first-century policy for multi-millennial climate and sea-level change. *Nature Climate Change* 6: 360–369.

Colin C, Duhamel M, Siani G et al. (2021) Changes in the intermediate water masses of the Mediterranean Sea during the last climatic cycle—New constraints from neodymium isotopes in Foraminifera. *Paleoceanography and Paleoclimatology* 36: e2020PA004153.

Conte M, Giuffrida A and Tedesco S (1989) The mediterranean oscillation: Impact on precipitation and hydrology in Italy. In: *Conference on Climate and Water*, pp. 121–137. Academy of Finland.

Debret M, Bout-Roumazeilles V, Grousset F et al. (2007) The origin of the 1500-year climate cycles in holocene north-Atlantic records. *Climate of the Past* 3: 569–575.

Desprat S, Combourieu-Nebout N, Essallami L et al. (2013) Deglacial and holocene vegetation and climatic changes in the southern central Mediterranean from a direct land–sea correlation. *Climate of the Past* 9: 767–787.

Di Rita F, Fletcher WJ, Aranbarri J et al. (2018) Holocene forest dynamics in central and western Mediterranean: Periodicity, spatio-temporal patterns and climate influence. *Scientific Reports* 8: 8929.

Dormoy I, Peyron O, Combourieu-Nebout N et al. (2009) Terrestrial climate variability and seasonality changes in the Mediterranean region between 15 000 and 4000 years BP deduced from marine pollen records. *Climate of the Past* 5: 615–632.

Duhamel M, Colin C, Revel M et al. (2020) Variations in eastern Mediterranean hydrology during the last climatic cycle as inferred from neodymium isotopes in foraminifera. *Quaternary Science Reviews* 237: 106306.

Dünkeloh A and Jacobeit J (2003) Circulation dynamics of Mediterranean precipitation variability 1948-98. *International Journal of Climatology* 23: 1843–1866.

Fach BA, Orek H, Yilmaz E et al. (2021) Water mass variability and levantine intermediate water formation in the Eastern Mediterranean between 2015 and 2017. *Journal of Geophysical Research Oceans* 126: e2020JC016472.

Fedele G, Mauri E, Notarstefano G et al. (2022) Characterization of the Atlantic water and levantine intermediate water in the Mediterranean Sea using 20 years of Argo data. *Ocean Science* 18: 129–142.

Fletcher WJ, Debret M and Goñi MFS (2013) Mid-holocene emergence of a low-frequency millennial oscillation in western Mediterranean climate: Implications for past dynamics of the North Atlantic atmospheric westerlies. *The Holocene* 23: 153–166.

Gasparini GP, Ortona A, Budillon G et al. (2005) The effect of the Eastern Mediterranean transient on the hydrographic characteristics in the Strait of Sicily and in the Tyrrhenian Sea. *Deep Sea Research Part I Oceanographic Research Papers* 52: 915–935.

Gouhier TC, Grinsted A and Simko V (2018) R package biwavelet: Conduct Univariate and Bivariate Wavelet Analyses (Version 0.20.17).

Hammer Harper DAT and Ryan PD (2001) PAST: Paleontological statistics software package for education and data analysis. *Palaeontologia Electronica* 4: 1–9.

Hennekam R, Jilbert T, Schnetger B et al. (2014) Solar forcing of Nile discharge and sapropel S1 formation in the early to middle Holocene eastern Mediterranean. *Paleoceanography* 29: 343–356.

Incarbona A and Sprovieri M (2020) The postglacial isotopic record of intermediate water connects Mediterranean sapropels and organic-rich layers. *Paleoceanography and Paleoclimatology* 35: e2020PA004009.

Jalut G, Esteban Amat A, Bonnet L et al. (2000) Holocene climatic changes in the western Mediterranean, from south-east France to south-east Spain. *Palaeogeography, Palaeoclimatology, Palaeoecology* 160: 255–290.

Jevrejeva S, Moore JC and Grinsted A (2003) Influence of the Arctic oscillation and El Niño-Southern Oscillation (ENSO) on ice conditions in the Baltic Sea: The wavelet approach. *Journal of Geophysical Research* 108(D21): 4677.

Jia G, Shevliakova E, Artaxo P et al. (2019) Land–climate interactions. In: Shukla PR, Skea J, Calvo Buendia E et al. (eds) *Climate Change and Land: An IPCC Special Report on Climate Change, Desertification, Land Degradation, Sustainable Land Management, Food Security, and Greenhouse Gas Fluxes in Terrestrial Ecosystems. IPCC AR6*, pp. 131–247.

Jury MR, Enfield DB and Mélice J (2002) Tropical monsoons around Africa: Stability of El Niño–Southern Oscillation associations and links with continental climate. *Journal of Geophysical Research Oceans* 107(C10): 15–17.

Juza M, Escudier R, Vargas-Yáñez M et al. (2019) Characterization of changes in western intermediate water properties enabled by an innovative geometry-based detection approach. *Journal of Marine Systems* 191: 1–12.

Juza M, Renault L, Ruiz S et al. (2013) Origin and pathways of winter intermediate water in the northwestern Mediterranean Sea using observations and numerical simulation. *Journal of Geophysical Research Oceans* 118: 6621–6633.

Lascaratos A, Williams RG and Tragou E (1993) A mixed-layer study of the formation of levantine intermediate water. *Journal of Geophysical Research Oceans* 98: 14739–14749.

Le Houedec S, Mojtahid M, Bicchi E et al. (2020) Suborbital hydrological variability inferred from coupled benthic and planktic foraminiferal-based proxies in the southeastern Mediterranean during the last 19 ka. *Paleoceanography and Paleoclimatology* 35: e2019PA003827.

Le Houedec S, Mojtahid M, Ciobanu M et al. (2021) Deglacial to holocene environmental changes in the northern Ligurian Sea: The dual influence of regional climate variability and large-scale intermediate Mediterranean circulation. *Palaeogeography, Palaeoclimatology, Palaeoecology* 576: 110500.

Lermusiaux PFJ and Robinson AR (2001) Features of dominant mesoscale variability, circulation patterns and dynamics in the Strait of Sicily. *Deep Sea Research Part I Oceanographic Research Papers* 48: 1953–1997.

Magny M, Combourieu-Nebout N, de Beaulieu JL et al. (2013) North–south palaeohydrological contrasts in the central Mediterranean during the holocene: Tentative synthesis and working hypotheses. *Climate of the Past* 9: 2043–2071.

Martrat B, Grimalt JO, Lopez-Martinez C et al. (2004) Abrupt temperature changes in the western Mediterranean over the past 250,000 years. *Science* 306: 1762–1765.

Masson-Delmotte V, Zhai P, Pirani A et al. (2021) *IPCC, 2021: Climate Change 2021: The Physical Science Basis. Contribution of Working Group I to the Sixth Assessment Report of the Intergovernmental Panel on Climate Change*. Cambridge and New York: Cambridge University Press.

McManus JF, Oppo DW and Cullen JL (1999) A 0.5-million-year record of millennial-scale climate variability in the North Atlantic. *Science* 283: 971–975.

MedECC (2020) Climate and Environmental Change in the Mediterranean Basin – Current Situation and Risks for the Future. First Mediterranean Assessment Report, Zenodo. DOI: 10.5281/zenodo.4768833

Millot C (1999) Circulation in the western Mediterranean Sea. *Journal of Marine Systems* 20: 423–442.

Millot C and Taupier-Letage I (2005) Circulation in the Mediterranean Sea. In: Saliot A (ed.) *The Mediterranean Sea, Handbook of Environmental Chemistry*. Berlin, Heidelberg: Springer, pp.29–66.

Mirzabaev A, Wu J, Evans J et al. (2019) Desertification. In: Shukla PR, Skea J, Calvo Buendia E et al. (eds) *Climate*

Change and Land: An IPCC Special Report on Climate Change, Desertification, Land Degradation, Sustainable Land Management, Food Security, and Greenhouse Gas Fluxes in Terrestrial Ecosystems. IPCC AR6, pp. 249–343.

Mojtahid M, Manceau R, Schiebel R et al. (2015) Thirteen thousand years of southeastern Mediterranean climate variability inferred from an integrative planktic foraminiferal-based approach. *Paleoceanography* 30: 402–422.

Moreno A, Cacho I, Canals M et al. (2005) Links between marine and atmospheric processes oscillating on a millennial timescale. A multi-proxy study of the last 50,000yr from the Alboran Sea (Western Mediterranean Sea). *Quaternary Science Reviews* 24: 1623–1636 (Quaternary Land-Ocean Correlation).

Morley A, Rosenthal Y and DeMenocal P (2014) Ocean-atmosphere climate shift during the mid-to-late holocene transition. *Earth and Planetary Science Letters* 388: 18–26.

Naughton F, Sánchez Goñi MF, Kageyama M et al. (2009) Wet to dry climatic trend in north-western Iberia within Heinrich events. *Earth and Planetary Science Letters* 284: 329–342.

O'Brien SR, Mayewski PA, Meeker LD et al. (1995) Complexity of holocene climate as reconstructed from a Greenland ice core. *Science* 270: 1962–1964.

Paillard D, Labeyrie L and Yiou P (1996) Macintosh program performs time-series analysis. *Eos Transactions American Geophysical Union* 77: 379–379.

Palutikof JP, Conte M, Casimiro Mendes J et al. (1996) Climate and climate change. In: Jane Brandt C and Thornes JB (eds) *Mediterranean Desertification and Land Use*. London: Wiley, pp.43–86.

Petrenko AA (2003) Variability of circulation features in the Gulf of Lion NW Mediterranean Sea. Importance of inertial currents. *Oceanologica Acta* 26: 323–338.

Peyron O, Goring S, Dormoy I et al. (2011) Holocene seasonality changes in the central Mediterranean region reconstructed from the pollen sequences of Lake accesa (Italy) and Tenaghi Philippon (Greece). *The Holocene* 21: 131–146.

Pinardi N, Cessi P, Borile F et al. (2019) The Mediterranean Sea overturning circulation. *Journal of Physical Oceanography* 49(7): 1699–1721.

R Core Team (2020) R: A language and environment for statistical computing [WWW document]. Available at: https://www.r-project.org/ (accessed 15 June 2021).

Regattieri E, Zanchetta G, Isola I et al. (2019) Holocene critical zone dynamics in an Alpine catchment inferred from a speleothem multiproxy record: disentangling climate and human influences. *Scientific Reports* 9: 17829.

Reimer PJ, Austin WEN, Bard E et al. (2023) The IntCal20 northern hemisphere radiocarbon age calibration curve (0–55 cal kBP). *Radiocarbon* 62: 725–757.

Reimer PJ and McCormac FG (2002) Marine radiocarbon reservoir corrections for the Mediterranean and Aegean Seas. *Radiocarbon* 44: 159–166.

Rigozo NR, Nordemann DJR, Souza Echer MP et al. (2007) Solar activity imprints in tree ring width from Chile (1610–1991). *Journal of Atmospheric and Solar-Terrestrial Physics* 69(9): 1049–1056.

Roberts N, Moreno A, Valero-Garcés BL et al. (2012) Palaeolimnological evidence for an east–west climate see-saw in the Mediterranean since AD 900. *Global and Planetary Change* 84–85: 23–34 (Perspectives on Climate in Medieval Time).

Rodrigo-Gámiz M, Martínez-Ruiz F, Rodríguez-Tovar FJ et al. (2014) Millennial- to centennial-scale climate periodicities and forcing mechanisms in the westernmost Mediterranean for the past 20,000 yr. *The Quaternary Research (Daiyonki-Kenkyu)* 81: 78–93.

Rohling EJ, Marino G and Grant KM (2015) Mediterranean climate and oceanography, and the periodic development of anoxic events (sapropels). *Earth-Science Reviews* 143: 62–97.

Salat J and Font J (1987) Water mass structure near and offshore the Catalan coast during the winters of 1982 and 1983. *Annales Geophysicae, Series B 5* B(1): 49–54.

Sánchez Goñi MF, Landais A, Fletcher WJ et al. (2008) Contrasting impacts of Dansgaard–Oeschger events over a western European latitudinal transect modulated by orbital parameters. *Quaternary Science Reviews* 27: 1136–1151.

Schroeder K, Chiggiato J, Bryden HL et al. (2016) Abrupt climate shift in the western Mediterranean Sea. *Scientific Reports* 6: 23009.

Shackleton NJ, Hall MA and Vincent E (2000) Phase relationships between millennial-scale events 64,000–24,000 years ago. *Paleoceanography* 15: 565–569.

Sierro FJ, Hodell DA, Curtis JH et al. (2005) Impact of iceberg melting on Mediterranean thermohaline circulation during Heinrich events. *Paleoceanography* 20: PA2019.

Sirocko F, Garbe-Schönberg D, McIntyre A et al. (1996) Teleconnections between the subtropical monsoons and high-latitude climates during the last deglaciation. *Science* 272: 526–529.

Skliris N (2014) Past, present and future patterns of the thermohaline circulation and characteristic water masses of the Mediterranean Sea. In: Goffredo S and Dubinsky Z (eds) *The Mediterranean Sea: Its History and Present Challenges*. Dordrecht: Springer, pp.29–48.

Sprovieri M, Di Stefano E, Incarbona A et al. (2012) Centennial-to millennial-scale climate oscillations in the central-eastern Mediterranean Sea between 20,000 and 70,000 years ago: Evidence from a high-resolution geochemical and micropaleontological record. *Quaternary Science Reviews* 46: 126–135.

Stocker TF, Qin D, Plattner GK et al. (2013) *IPCC, 2013: Climate Change 2013: The Physical Science Basis. Contribution of Working Group I to the Fifth Assessment Report of the Intergovernmental Panel on Climate Change*. In: Stocker TF, Qin GKP, Tignor M, et al. (eds) IPCC AR5, pp. 1535.

Theocharis A, Klein B, Nittis K et al. (2002) Evolution and status of the Eastern Mediterranean Transient (1997–1999). *Journal of Marine Systems* 33–34: 91–116.

Toucanne S, Jouet G, Ducassou E et al. (2012) A 130,000-year record of levantine intermediate water flow variability in the Corsica Trough, western Mediterranean Sea. *Quaternary Science Reviews* 33: 55–73.

Tsimplis MN and Bryden HL (2000) Estimation of the transports through the Strait of Gibraltar. *Deep Sea Research Part I Oceanographic Research Papers* 47: 2219–2242.

Vargas JM, García-Lafuente J, Candela J et al. (2006) Fortnightly and monthly variability of the exchange through the Strait of Gibraltar. *Progress in Oceanography* 70: 466–485 (Gabriel T. Csanady: *Understanding the Physics of the Ocean*).

Vargas-Yáñez M, García-Martínez MC, Moya F, et al. (2017) Updating temperature and salinity mean values and trends in the Western Mediterranean: The RADMED project. *Progress in Oceanography* 157: 27–46.

Wüst G (1961) On the vertical circulation of the Mediterranean Sea. *Journal of Geophysical Research* 66: 3261–3271.

Zanchetta G, Bar-Matthews M, Drysdale RN et al. (2014) Coeval dry events in the central and eastern Mediterranean basin at 5.2 and 5.6ka recorded in Corchia (Italy) and Soreq caves (Israel) speleothems. *Global and Planetary Change* 122: 130–139.

Zanchetta G, Drysdale RN, Hellstrom JC et al. (2007) Enhanced rainfall in the western Mediterranean during deposition of sapropel S1: Stalagmite evidence from Corchia cave (Central Italy). *Quaternary Science Reviews* 26: 279–286.

Zanchetta G, Sulpizio R, Roberts N et al. (2011) Tephrostratigraphy, chronology and climatic events of the Mediterranean basin during the holocene: An overview. *The Holocene* 21: 33–52.